Anal. Chem. **2002,** *74,* 3134−3141

Evaluation of the Separate Equilibrium Processes That Dictate the Upper Detection Limit of Neutral Ionophore-Based Potentiometric Sensors

Yu Qin and Eric Bakker*

Department of Chemistry, Auburn University, Auburn, Alabama 36849

The upper detection limit of polar ionophore-based ion-selective electrode membranes is predicted by utilizing the coextraction constant of dissociated electrolyte, the stability constant of the ionophore, and the membrane composition. The coextraction constant of dissociated electrolytes into the polar poly(vinyl chloride) membrane plasticized with *o*-nitrophenyl octyl ether (PVC−NPOE) is here measured by a novel approach. The sandwich membrane technique is utilized, with one membrane segment containing a lipophilic cation exchanger and the other containing an anion exchanger. This yields information about the coextraction constant and the free ion concentrations of the electrolyte in the two segments. Predictions correlate quantitatively with the upper detection limit observed for ion-selective electrodes based on the ionophores valinomycin, *tert*-butylcalix[4]arene tetraethyl ester, and calcimycin. The difficulties of the prediction of the upper detection limit for nonpolar poly(vinyl chloride) membranes plasticized with bis(2-ethylhexyl sebacate) (PVC−DOS) due to ion association are discussed in detail. A thermodynamic cycle experiment with a series of sandwich membranes shows that the principal processes governing the upper detection limit of PVC−DOS membranes are identical to those for the PVC−NPOE membranes. However, the stability of the ion pairs between the ionophore−metal ion complexes and the extracted anion are different from that of ion pairs formed between the same anion and the lipophilic anion exchanger. This makes it difficult to quantitatively predict the upper detection limit on the basis of simple apparent coextraction and complexation data alone. The approach reported herein is useful not only for mechanistic purposes but also to shed light onto the many cases where coextraction effects need to be understood but are not directly experimentally accessible.

In recent years, important progress has been reported on how co-ion interference of ion-selective electrodes (ISEs) can be described[1,2] and how experiments need to be performed to reveal the true ion-exchange selectivity of such membranes.[3,4] To significantly improve the response of ISEs, such as the lower detection limit,[4−7] it is imperative that all ion-exchange and electrolyte coextraction equilibria are well understood. Even ion disturbances on the order of fractions of a percent on the inner membrane side can lead to significant changes in the observed detection limit.[8] Since such small changes are difficult to measure, theoretical models are required to calculate these processes as accurately as possible.

Ion-exchange processes have always been an important focus in the field of ion-selective electrodes, since they ordinarily dictate whether a sensor can be used in a sample that contains a given level of interfering ions. In contrast, coextraction effects have historically been studied in much less detail. It is well established that the upper detection limit of ISEs is dictated by coextraction of electrolyte into the organic phase, thereby exceeding the ion-exchange capability of the membrane.[9−12] If an ionophore is present in the membrane, the extraction of electrolyte is mediated by the ionophore because complexation of one ion takes place in the organic phase. This mediated extraction will continue to occur with increasing sample concentration until all ionophore in the organic-phase boundary is present in its complexed form.[13] It has been shown that this situation should render a cation-selective membrane anion responsive, because the complexed ionophore now acts as a nonspecific anion exchanger.[14] Therefore, the upper detection limit can be described as the intercept of both extrapolated linear segments of the calibration curve.[14]

This paper presents a more careful, quantitative insight into the individual thermodynamic parameters that dictate the upper detection limit of ion-selective electrodes. The discussion first deals

(1) Nägele, M.; Bakker, E.; Pretsch, E. *Anal. Chem.* **1999**, *71*, 1041.
(2) Bakker, E.; Pretsch, E.; Bühlmann, P. *Anal. Chem.* **2000**, *72*, 1127.
(3) Bakker, E. *Anal. Chem.* **1997**, *69*, 1061.
(4) Sokalski, T.; Ceresa, A.; Zwickl, T.; Pretsch, E. *J. Am Chem. Soc.* **1997**, *119*, 11347.
(5) Sokalski, T.; Ceresa, A.; Fibbioli, M.; Zwickl, T.; Bakker, E.; Pretsch, E. *Anal. Chem.* **1999**, *71*, 1210.
(6) Qin, W.; Zwickl, T.; Pretsch, E. *Anal. Chem.* **2000**, *72*, 3236.
(7) Ceresa, A.; Bakker, E.; Hattendorf, B.; Günther, D.; Pretsch, E. *Anal. Chem.* **2001**, *72*, 343.
(8) Bakker, E.; Pretsch, E. *Trends Anal. Chem.* **2001**, *20*, 11.
(9) Morf, W. E.; Kahr, G.; Simon, W. *Anal. Lett.* **1974**, *7*, 9.
(10) Buck, R. P.; Toth, K.; Gràf, E.; Horvai, G.; Pungor, E. *J. Electroanal. Chem.* **1987**, *223*, 51.
(11) Buck, R. P.; Cosofret, V. V.; Lindner, E. *Anal. Chim. Acta* **1993**, *282*, 273.
(12) Bühlmann, P.; Amemiya, S.; Yajima, S.; Umezawa, Y. *Anal. Chem.* **1998**, *70*, 4291.
(13) Bakker, E.; Nägele, M.; Schaller, U.; Pretsch, E. *Electroanalysis* **1995**, *7*, 817.
(14) Bakker, E.; Xu, A.; Pretsch, E. *Anal. Chim. Acta* **1994**, *295*, 253.

10.1021/ac0156159 CCC: $22.00
Published on Web 05/09/2002

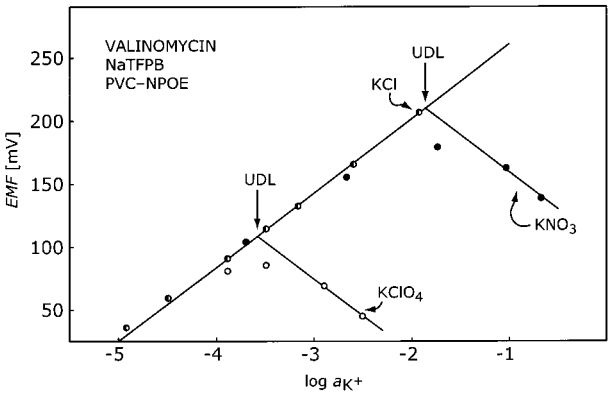

Figure 1. Experimental upper detection limits of PVC−NPOE membranes containing 20 mmol kg^{-1} valinomycin and 5 mmol kg^{-1} lipophilic anionic additive NaTFPB in contact with different concentrations of KCl, KNO_3, and $KClO_4$ in the sample. The upper detection limit is given as the intercept of the two extrapolated linear segments of each calibration curve, as indicated.

with polar membrane phases, where theory can be simplified since ion pairing may be neglected and the upper detection limit of ion-selective membranes can be quite easily predicted. Experiments are then performed to describe the more complex nonpolar membrane phases where these assumptions do not hold. The new segmented sandwich membrane technique,[15,16] normally used to assess complex formation constants,[16,17] is adapted here to characterize electrolyte coextraction behavior into membranes.

THEORY

Modeling the Upper Detection Limit. The theoretical treatment presented here focuses on polymeric membrane materials where ion-pairing effects can be neglected. It utilizes the traditional definition of the upper detection limit as the intersection of the two extrapolated linear portions of the calibration curve, in complete analogy to the established definition of the lower detection limit.[18] For cation-selective ionophore-based membrane electrodes, for example, it is known that the electrode slope eventually changes from a Nernstian cation slope to an ideally Nernstian anion slope, owing to the saturation of ionophore due to coextracting sample electrolyte.[11,12,14] This is strictly speaking a special case.[19] At high sample concentrations, the complexed ionophore acts effectively as a nonspecific ion exchanger for anions, which leads to an anionic response slope. This general process is shown in Figure 1. The two regions of the calibration curve can be described with two separate Nernst equations, one for the cation response region

$$E_I = K_I + (RT/z_IF) \ln a_I \quad (1)$$

and one for the anion response region

$$E_A = K_A - (RT/z_AF) \ln a_A \quad (2)$$

where a_I and a_A are the sample activity of the cation I and anion A with charge z_{I^+} and z_{A^-}, and R, T, and F have their established meanings. The upper detection limit, a_I(UDL), is then given by setting both potentials equal:

$$\ln a_I(\mathrm{UDL}) = \frac{z_IF}{RT}(K_A - K_I) - \frac{z_I}{z_A} \ln a_A \quad (3)$$

This theory is now extended to reflect the relevant equilibrium processes that dictate the upper detection limit of ISEs. A simpler version of this was presented earlier for H^+-responsive systems[14] and is here expanded to respect for any ionic charge and complex stoichiometry.

Generally, the phase boundary potential E_I at the sample−membrane side can be described as

$$E_I = (RT/z_IF) \ln(a_Ik_I/[I^{z_I+}]) \quad (4)$$

where k_I incorporates the free energy of transfer for the ion I and $[I^{z_I+}]$ is the concentration of uncomplexed ion in the membrane phase boundary in contact with the sample. For a cation-selective electrode that responds with a Nernstian electrode slope to changes in a_I, $[I^{z_I+}]$ must be constant.[13] This is established by a lipophilic ion exchanger in the membrane and the lack of interference by competing cations or coextracting anions. In a more concentrated sample, coextraction may render the membrane anion responsive. In this case, eq 1 can be written for this portion of the calibration in complete analogy for anions to give

$$E_A = -(RT/z_AF) \ln(a_Ak_A/[A^{z_A-}]) \quad (5)$$

Again, the concentration of uncomplexed anions in the membrane phase boundary, $[A^{z_A-}]$, must be independent of a_A to yield a Nernstian anion slope. At the upper detection limit, eqs 4 and 5 must be equal (intersection), which yields

$$a_I(\mathrm{UDL}) = \frac{[I^{z_I+}]}{k_I}\left(\frac{a_Ak_A}{[A^{z_A-}]}\right)^{-z_I/z_A} \quad (6)$$

As mentioned above, the phase boundary concentrations $[I^{z_I+}]$ and $[A^{z_A-}]$ are sample independent terms for the two different portions of the calibration curve that each give a Nernstian response slope. Often, calibration curves are not recorded in a constant ionic background, but in incremental concentrations of an electrolyte $I_{z_A}A_{z_I}$. In that case, the anion activity is a direct function of the cation activity, and eq 6 is rewritten as

$$a_I(\mathrm{UDL}) = \left\{\left(\frac{[I^{z_I+}]}{k_I}\right)^{1/z_I}\left(\frac{z_A[A^{z_A-}]}{z_Ik_A}\right)^{1/z_A}\right\}^{z_Az_I/(z_A+z_I)} \quad (7)$$

Assuming that ion pairs can be neglected in the organic phase, the two unknowns $[I^{z_I+}]$ and $[A^{z_A-}]$ are now expressed by experimentally accessible parameters.

(15) Mikhelson, K. N. *Sens. Actuators, B* **1994**, *18−19*, 31.
(16) Mi, Y.; Bakker, E. *Anal. Chem.* **1999**, *71*, 5279.
(17) Qin, Y.; Mi, Y.; Bakker, E. *Anal. Chim. Acta* **2000**, *421*, 207.
(18) Guilbault, G. G.; Durst, R. A.; Frant, M. S.; Freiser, H.; Hansen, E. H.; Light, T. S.; E. Pungor; Rechnitz, G.; Rice, N. M.; Rohm, T. J.; Simon, W.; Thomas, J. D. R. *Pure Appl. Chem.* **1976**, *48*, 127.
(19) Boles, J. H.; Buck, R. P. *Anal. Chem.* **1973**, *45*, 2057.

In the membrane phase, the primary ion $[I^{z_I+}]$ may be complexed by an ionophore L with a 1:n complex stoichiometry, with the stability constant

$$\beta_n = [IL_n^{z_I+}]/[I^{z_I+}][L]^n \quad (8)$$

In addition, the charge balance in the anion response region is now written as $[A^{z_A-}] = z_I L_T/(z_A n)$, where L_T is the total ionophore concentration. In analogy, the cation response region has the charge balance $[IL^{z_I+}] = z_I R_T$ and mass balance $[L] = L_T - z_I R_T/n$, where R_T is the total cation-exchanger concentration in the membrane with a charge of -1. These relationships, including eq 8 to replace $[I^{z_I+}]$, are inserted into eq 7 to give an explicit relationship between the upper detection limit and the complex formation constant and free energy of ion transfer as relevant thermodynamic parameters that dictate this process:

$$a_I(\mathrm{UDL}) = \left\{\frac{1}{k_I^{1/z_I} k_A^{1/z_A}}\left(\frac{z_I R_T}{\beta_n (L_T - z_I R_T/n)^n}\right)^{1/z_I}\left(\frac{nL_T - z_I R_T}{n^2}\right)^{1/z_A}\right\}^{z_A z_I/(z_A+z_I)} \quad (9)$$

For the simple case of monovalent anions and cations, and for a complex stoichiometry of $n = 1$, eq 9 simplifies to the known equation[20]

$$a_I(\mathrm{UDL}) = (R_T/k_I k_A \beta_1)^{1/2} \quad (10)$$

Equation 9 makes it clear that two thermodynamic parameters are required in addition to the known membrane composition. The first is the complex formation constant, β_n, for which a number of experimental methods are today available. The second is the coextraction constant, $k_I^{1/z_I} k_A^{1/z_A}$, for which no established method is known thus far. There is only some indirect information in the literature about the coextraction constant of dissociated electrolyte. The value for the KCl extraction constant into PVC−DOS, for example, has been estimated to be $\sim 10^{-10}$ by modeling the measuring range of ionophore-based pH electrodes.[21] Another indirect indication for the coextraction constants of electrolyte comes from voltammetric experiments on ionophore-free ion-selective electrode membranes without ion-exchanger properties, but with a high concentration of inert lipophilic electrolyte.[22] The observed potential window is limited by extraction of cations at one potential extreme and of anions on the other. A typical potential window of ~1590 mV gave an estimated coextraction constant for NaCl of $\sim 10^{-9.6}$ with PVC−NPOE as membrane material. The next section introduces a new, more quantitative method for the estimation of such electrolyte coextraction constants. If the coextraction constant for one chosen electrolyte and a given membrane matrix is known, the corresponding value for other electrolytes can be calculated with experimental selectivity coefficients K_{IJ}^{pot} of membranes containing only a dissociated ion exchanger:[23]

$$K_{IJ}^{pot} = (R_T/k_I z_I)(k_J z_J/R_T)^{z_I/z_J} \quad (11)$$

where I is the ion for which k_I is known and J is the ion for which it is desired.

Determining Electrolyte Coextraction Constants. The driving force to extract hydrophilic electrolyte is here, for the first time, assessed with the sandwich membrane method. One membrane segment contains a lipophilic cation exchanger, and the other contains an equal concentration of lipophilic anion exchanger. The membrane potential of the resulting sandwich should be the sum of the two individual phase boundary potentials. Since one side is cation and the other anion responsive, the potential is written for monovalent ions as

$$E_M = \frac{RT}{F}\ln\frac{[A^-]}{k_A a_A}\frac{[I^+]'}{k_I a_I'} \quad (12)$$

where the prime indicates the composition at the inner phase boundary. This equation is an approximation since it neglects the membrane junction potential at the place where the two segments are fused together. The estimated error from this approximation is no more than 10 mV, which is deemed acceptable. For a polar, ionophore-free membrane, the uncomplexed concentrations of cations and anions in both segments can be approximated by the concentration of ion exchanger at each side. Since both concentrations are equal (R_T), eq 12 yields directly the desired coextraction constant as the product $k_I k_A$:

$$E_M = -\frac{2.303RT}{F}\log(k_I k_A a_I' a_A) + 2\frac{2.303RT}{F}\log R_T \quad (13)$$

For a plot of E_M versus log R_T at a constant, known composition of sample and inner electrolyte, theory predicts a double Nernstian slope. A fit of the data with eq 13 yields coextraction constants, k_I k_A, that can be inserted into eq 10 for the prediction of upper detection limits where membrane ion pairing is neglectable.

Thermodynamic Cycle with Sandwich Membrane Experiments. This section introduces a semiquantitative approach to evaluate the individual thermodynamic processes that dictate the upper detection limit of ISEs if membrane ion pairing cannot be neglected. As established above (eq 3), the upper detection limit is given by the measurement of two different membrane equilibrium compositions, one where interference is absent (Nernstian cation slope) and one where all ionophore molecules are essentially in their complexed form (Nernstian anion slope). One can yield the same information by performing a sandwich membrane experiment where each segment contains one of the two desired compositions. For $KClO_4$ interference, for example, the sandwich membrane can be described with standard cell notation as

(20) Mathison, S.; Bakker, E. *Anal. Chem.* **1998**, *70*, 303.
(21) Bakker, E.; Bühlmann, P.; Pretsch, E. *Chem. Rev.* **1997**, *97*, 3083.
(22) Jadhav, S.; Bakker, E. *Anal. Chem.* **1999**, *71*, 3657.
(23) Bakker, E.; Meruva, R. K.; Pretsch, E.; Meyerhoff, M. E. *Anal. Chem.* **1994**, *66*, 3021.

$$KCl(aq) \,||\, KL^+(org), R^-(org), L(org) \,|\, KL^+(org), R^-(org), ClO_4^-(org) \,||\, KClO_4(aq) \quad (14)$$

The double vertical bars denote the membrane−water phase boundary, while the single vertical bar symbolizes the interface between both segments. The membrane potential for the experiment depicted in eq 14, with the aqueous ion activities extrapolated to 1 M, is expected to be identical to the term ($K_A - K_I$) in eq 3. This general process can be described with the following chemical equation:

$$K^+(aq) + L(org) + ClO_4^-(aq) \rightarrow KL^+ClO_4^-(org) \quad (15)$$

The purpose of the sandwich experiment is to construct a thermodynamic cycle of individual measurements that can each be directly evaluated. Here, the practical case of valinomycin membranes undergoing potassium perchlorate interference is used as an example. Equation 15 is broken into three different processes that are described with the following chemical equations:

$$K^+(aq) + R^+R^-(org) + ClO_4^-(aq) \rightarrow K^+R^-(org) + R^+ClO_4^-(org) \quad (16)$$

$$K^+R^-(org) + L(org) \rightarrow KL^+R^-(org) \quad (17)$$

$$R^+ClO_4^-(org) + KL^+R^-(org) \rightarrow KL^+ClO_4^-(org) + R^+R^-(org) \quad (18)$$

Summation of the three equations gives eq 15.

Each of these separate equilibrium processes is evaluated by a separate sandwich membrane experiment. The first evaluates the apparent extent of coextraction of noncomplexed electrolyte $KClO_4$ into PVC−DOS. The corresponding sandwich membrane experiment for eq 16 is written with the following cell notation:

$$KCl(aq) \,||\, K^+(org), R^-(org) \,|\, R^+(org), ClO_4^-(org) \,||\, KClO_4(aq) \quad (19)$$

Note that K^+ and ClO_4^- are extracted into different membrane segments and do not directly interact with one another, as written in eq 16.

The second experiment (eq 17) is a measure of the extent of complexation of K^+ by the ionophore, and the corresponding sandwich membrane experiment is denoted as

$$KCl(aq) \,||\, KL^+(org), R^-(org), L(org) \,|\, K^+(org), R^-(org) \,||\, KCl(aq) \quad (20)$$

Note that the right side of eq 20 is identical to the left side of eq 19. Summation of the two potentials eliminates this term.

The third equilibrium (eq 18) links the previous two processes (eqs 16 and 17) to the overall equilibrium 15. It takes into account the difference in ion pairing between perchlorate and either the anion exchanger R^+ or the potassium complex KL^+. This equilibrium is evaluated in the following sandwich membrane experiment:

$$KClO_4(aq) \,||\, R^+(org), ClO_4^-(org) \,|\, KL^+(org), R^-(org), ClO_4^-(org) \,||\, KClO_4(aq) \quad (21)$$

Summing eqs 19, 20, and 21 should give the same overall potential that dictates the process of anion interference (eq 14), which was shown above to be identical to ($K_A - K_I$) in eq 3. Therefore, each individual sandwich membrane potential must be indicative of the driving force of a major thermodynamic process that dictates the upper limit of detection. Equation 19 describes the extent of coextraction, eq 20 the extent of ion complexation, and eq 21 evaluates the influence of membrane ion pairing.

EXPERIMENTAL SECTION

Reagents. Sodium tetrakis[3,4-bis(trifluoromethyl)phenyl]borate (NaTFPB), tridodecylmethylammonium chloride (TDMACl),), *tert*-butylcalix[4]arene tetraethyl ester (Na-4), calcimycin (Ca-4), bis(2-ethylhexyl) sebacate (DOS), *o*-nitrophenyl octyl ether (NPOE), high molecular weight poly(vinyl chloride) (PVC), tetrahydrofuran (THF), and all salts were purchased in Selectophore or puriss quality from Fluka Chemical Corp. (Milwaukee, WI). Valinomycin (K-1) was purchased from Sigma in HPLC grade. Aqueous solutions were prepared by dissolving the appropriate salts in Nanopure purified water.

Electrode Setup. If not otherwise noted, ion-selective electrode membranes were cast by weighing out the ionophore (20 mmol kg^{-1}, if used), NaTFPB (5 mmol kg^{-1}, if used), TDMACl (5 mmol kg^{-1}, if used), together with PVC and the plasticizer DOS or o-NPOE (1:2 by weight), to give a total cocktail mass of 140 mg, dissolving the mixture in 1.5 mL of THF, and pouring it into a glass ring (2.2-cm i.d.) affixed with rubber bands onto a microscope glass slide. The solvent THF was allowed to evaporate overnight to form the parent membranes. A series of 6-mm-diameter disks were then cut with a cork borer from the parent membrane and mounted in IS-561 Philips electrode bodies (Moeller, Zurich, Switzerland). All membrane electrode potential measurements were performed at laboratory ambient temperature in unstirred salt solutions (identical to the conditioning solution) versus an Ag/AgCl reference electrode with a 1 M LiOAc bridge electrolyte. The potential was recorded as the average of the last minute of measurement of a 5-min measurement period.

Upper Detection Limit Measurements. The inner filling solution of the electrodes consisted of 10^{-3} M chloride salt of the primary cation (K^+ for membranes containing valinomycin, Na^+ for Na-4, and Ca^{2+} for Ca-4). The membranes were conditioned overnight in a solution identical to the inner filling solution before measurement. The calibration curves of the electrodes were determined in separate solutions of a primary ion salt containing counteranions of different lipophilicity. The upper detection limit was determined by extrapolating the two linear segments of the calibration curve at high concentrations and determining the logarithmic cation activity at the intercept.

Sandwich Membrane Measurements. The membranes were conditioned overnight in the same solutions as the inner filling solution before mounting into an electrode configuration. For each

measurement, one disk was incorporated into a single chosen IS-561 Philips electrode body (Moeller). The body was selected to give a potential value that deviated less than 2 mV for different single-membrane disks. The sandwich membrane was made by fusing two individual membranes together with pressure from a metal spatula, right after blotting each of them dry with tissue paper. The obtained sandwich membrane was visibly controlled for air bubbles and then mounted in the same electrode body. The elapsed time between sandwich fusion and exposure to electrolyte was normally less than 1 min. The potential of such sandwich membranes remains free from diffusion-induced potential drifts for ~20 min. Standard deviations were obtained based on the measurements of sets of at least three replicate membrane disks that were made from the same parent membrane.

Determination of Coextraction Constants. The segment facing the 0.01 M KCl inner electrolyte was prepared with 5, 10, or 15 mmol kg^{-1} NaTFPB, while the segment facing the 0.01 M $KClO_4$ or 0.01 M KNO_3 sample contained TDMACl of equal molality. These experiments were performed with membranes containing the plasticizers NPOE and DOS. The experimental membrane potentials were inserted into eq 13 and solved for the logarithmic product of k_I and k_A to obtain the desired coextraction constant for the electrolyte $KClO_4$ or KNO_3 under study.

Sandwich Experiments for Nonpolar Membranes. All membrane segments contained PVC−DOS (1:2) as a model nonpolar membrane. Both membrane segments for the experiment depicted in eq 14 contained 5 mmol kg^{-1} NaTFPB and 20 mmol kg^{-1} valinomycin, with 10^{-3} M KCl inner solution and 10^{-1} M $KClO_4$ sample, and were individually conditioned in each solution before measurement. The segments for eq 19 contained 5 mmol kg^{-1} NaTFPB (inner side) and 5 mmol kg^{-1} TDMACl (outer side), with a 10^{-2} M KCl inner filling solution and a 10^{-2} M $KClO_4$ sample. For the experiment shown in eq 20, the inner segment was identical to that for eq 14, while the outer segment contained 5 mmol kg^{-1} NaTFPB. Both solutions were 10^{-2} M KCl. The inner segment for eq 21 consisted of 5 mmol kg^{-1} TDMACl, while the outer segment was identical to the one for eq 14. Both samples consisted of 10^{-2} M $KClO_4$. The segments to evaluate the difference in perchlorate ion pairing between the charged valinomycin−potassium complex and $TDMA^+$ consisted of 5 mmol kg^{-1} TDMACl (inner segment) and 5 mmol kg^{-1} valinomycin (outer segment), with 0.1 M $KClO_4$ for both solutions. Summations of the experimental potentials were performed after extrapolating to 1 M sample activities with the Nernst equation.

RESULTS AND DISCUSSION

The upper detection limit of ionophore-based potentiometric cation sensors is assumed to be dictated by the coextraction of dissociated sample electrolyte into the polymeric membrane phase and the complexation of the extracted cation by the ionophore.[9] Depending on the chemical nature of the membrane material and active sensing components, various additional ion-pairing and association constants may also contribute to the overall extraction equilibrium. For this reason, the polar matrix PVC−NPOE was first chosen as the simplest membrane material to evaluate the two mentioned principal processes.

Predicting the Upper Detection Limit of Polar Membranes. Recently, complex formation constants of various electrically neutral ionophores in two different membrane materials, PVC−DOS and PVC−NPOE, were determined with the so-called sandwich membrane method.[16,17] Here, two membranes of different composition are fused together and the resulting membrane potential is measured. Because the sandwich membrane is concentration-polarized, the potential gives information about the activity ratio of uncomplexed ion in both segments. If only one of the two segments contains the ionophore, for example, complex formation constants can be determined. Consequently, these previously determined values were utilized in this work.

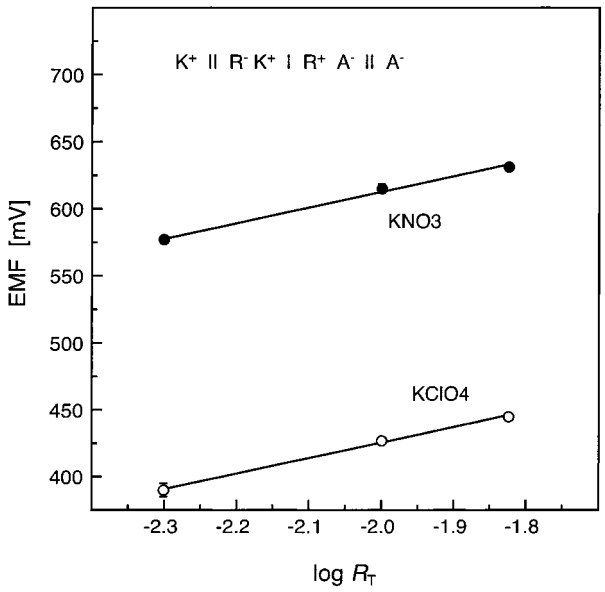

Figure 2. PVC−NPOE sandwich membrane potentials, with one side containing a cation exchanger and the other an anion exchanger of the same concentration, as a function of the indicated concentration of the ion-exchanger sites in the membrane. The double Nernstian slope is expected from theory (eq 13), while the intercept reflects the coextraction constant for the indicated electrolyte. Error bars shown are standard deviations from three replicate measurements and, in some cases, smaller than the plot symbols.

In this work, we attempted to perform a more accurate determination of the coextraction constant of dissociated electrolyte. A novel type of segmented sandwich membrane experiment was designed for this purpose. As described in the Theory section, one membrane segment contained a lipophilic cation exchanger and the other an equal concentration of lipophilic anion exchanger. The potential of the resulting fused sandwich membrane should give direct information about the coextraction constant (eq 13). For a plot of the membrane potential versus the logarithmic concentration of lipophilic ion exchanger in the segments at a constant composition of sample and inner electrolyte, theory predicts a double Nernstian slope. To confirm this theoretical relationship, a number of sandwich membrane experiments were performed with different ion-exchanger concentrations in both segments. The resulting membrane potentials are shown in Figure 2, and the slopes indeed nicely correspond to theory (116 mV $decade^{-1}$ for $KClO_4$ and 115 mV $decade^{-1}$ for KNO_3; theory, 117 mV $decade^{-1}$). From these experiments, log $k_I k_A$ was found to be -7.18 ± 0.04 for $KClO_4$ and -10.38 ± 0.02 for KNO_3. These coextraction constants are in agreement with the expectation that ion-selective electrode membranes are hydrophobic materials where small electrolytes are difficult to extract without mediation by an ionophore. Further, the difference between the two values

Table 1. Experimental Selectivity Coefficients for Ionophore-Free Ion-Exchanger Membranes Utilized for the Calculations Presented Here

cation J	log $K_{K,J}^{pot}$ [a]	anion J	log $K_{ClO4,J}^{pot}$ [b]
H^+	−1.5	SCN^-	−1.4
Na^+	−1.2	NO_2-	−4.1
K^+	0.0	ClO_4-	0.0
Ag^+	−0.2	I^-	−1.8
Mg^{2+}	−1.1	Br^-	−4.0
Ca^{2+}	−0.5	NO_3^-	−3.1
Cu^{2+}	−2.3	HCO_3^-	−6.6
Cd^{2+}	−2.2	Cl^-	−5.2
Pb^{2+}	−1.3	F^-	−7.1
		OAc^-	−6.7
		SO_4^{2-}	−6.9

[a] With PVC−NPOE membranes containing the cation exchanger NaTFPB.[25] [b] With PVC−NPOE membranes containing the anion exchanger TDMACl from ref 24.

Table 2. Coextraction Constants ($k_I^{1/z_I} k_A^{1/z_A}$; See Eq 9) from Water into PVC−NPOE for Electrolytes of the Indicated Cations and Anions, Calculated[23] with the Selectivity Coefficients Shown in Table 1 (see Eq 11) and with the Experimental Coextraction Constant Determined Here for $KClO_4$

	H^+	Na^+	K^+	Ag^+	Mg^{2+}	Ca^{2+}
SCN^-	−10.1	−9.8	−8.6	−8.8	−8.7	−8.1
NO_2^-	−12.8	−12.5	−11.3	−11.5	−11.4	−10.8
ClO_4^-	−8.7	−8.4	−7.2	−7.4	−7.3	−6.7
I^-	−10.5	−10.2	−9.0	−9.2	−9.1	−8.5
Br^-	−12.7	−12.4	−11.2	−11.4	−11.3	−10.7
NO_3^-	−11.8	−11.5	−10.3	−10.5	−10.4	−9.8
HCO_3^-	−15.3	−15.0	−13.8	−14.0	−13.9	−13.3
Cl^-	−13.9	−13.6	−12.4	−12.6	−12.5	−11.9
F^-	−15.8	−15.5	−14.3	−14.5	−14.4	−13.8
OAc^-	−15.4	−15.1	−13.9	−14.1	−14.0	−13.4
SO_4^{2-}	−14.9	−14.6	−13.4	−13.6	−13.5	−12.9

Table 3. Predicted Upper Detection Limits for PVC−NPOE Membranes Containing 20 mmol kg^{-1} Ionophore and 5 mmol kg^{-1} Lipophilic Ion Exchanger in Contact with the Listed Sample Primary Cation−Anion Salt, Calculated with Coextraction Data from Table 2 and with Eq 9

				loga_I(UDL)		
ionophore[a]	z_I	n[b]	logβ_n[c]	Cl^-	NO_3^-	ClO_4^-
K-1	1	1	11.6	−0.8	−1.8	−3.4
K-2	1	1	10.0	0.0	−1.0	−2.6
K-3	1	1	10.2	−0.1	−1.1	−2.7
Na-1	1	2	9.4	1.7	0.6	−0.9
Na-2	1	2	10.9	0.9	−0.1	−1.7
Na-3	1	1	9.2	1.0	0.0	−1.6
Na-4	1	1	10.3	0.5	−0.6	−2.1
Ca-4	2	2	12.9	2.8	1.4	−0.7

[a] Notation of ionophores are as in ref 17. [b] n is the assumed complex stoichiometry. [c] Complex formation constants in PVC−NPOE as determined previously.[17]

is consistent with the known selectivity coefficient for an anion-exchanger membrane (log $K_{NO_3,ClO_4}^{pot} = 3.0$).[24] It is more difficult to extract nitrate into an ion-exchanger membrane than perchlorate.

These individual values can now be utilized to predict the upper detection limit of ionophore-based ion-selective electrodes. Figure 1 shows the response of a valinomycin-based potassium ISE to varying $KClO_4$ sample concentrations. The detection limit is indicated in the plot and is found to be log a_K(UDL) = −3.6. Valinomycin is known to form 1:1 complexes with potassium. The upper detection limit can therefore be predicted from thermodynamic parameters with the simplified eq 10. Indeed, inserting the complex formation constant in PVC−NPOE (log $\beta_1 = 11.63 \pm 0.08$) and the coextraction constant for dissociated $KClO_4$ (log $k_K k_{ClO_4} = -7.18 \pm 0.04$), together with the cation-exchanger concentration of the membrane ($R_T = 0.005$ mol kg^{-1}), gives an upper detection limit of log a_K(UDL) = −3.37 ± 0.09, which agrees well with the experiment shown in Figure 1.

It appears that the upper detection limit of ionophore-based PVC−NPOE membranes can be predicted satisfactorily by knowing just two thermodynamic parameters, the complex formation and electrolyte coextraction constant, in addition to the membrane composition. The former can be determined with the segmented sandwich membrane method for each ionophore, while the latter is characteristic for the membrane material and the nature of the electrolyte. If these simple assumptions are valid, the coextraction data determined here can be applied to other anions and cations. Table 2 presents log $k_I^{1/zI} k_A^{1/zA}$ values for PVC−NPOE as predicted from the data obtained here and by inserting known selectivity coefficients[24,25] for ionophore-free ion-exchanger membranes (see Table 1) into eq 11. Consequently, Table 3 predicts the upper detection limit for various membrane electrodes for which the ionophore complex formation constant has been determined in PVC−NPOE,[17] calculated with data from Table 2 and with eq 9. For example, the upper detection limit for a valinomycin membrane in contact with potassium nitrate solutions nicely matches the experiment shown in Figure 1. In addition, Na-4- and Ca-4-based PVC−NPOE membranes were measured in solutions containing the perchlorate salts of sodium and calcium, respectively. The experimental upper detection limits were −1.95 and −0.35 M, respectively (data not shown), which also compare very well to the calculated values shown in Table 3 (−2.1 and −0.7 M, respectively). For some membrane electrodes shown in Table 3, the predicted upper detection limit is clearly too high to be observed directly. Indeed, there are applications where even a small extent of coextraction plays a very important role in ISE function, especially in view of minimizing the detection limit.[26] The approach presented here may therefore yield information for modeling and optimization purposes of such cases.

Predicting the Upper Detection Limit of Nonpolar (PVC−DOS) Membranes. The prediction of the upper detection limit for nonpolar membrane phases may be more difficult, since ion associations in such environments are expected to be strong. Indeed, the simple equation applied to PVC−NPOE fails with the nonpolar membrane material PVC−DOS. The apparent log $k_I k_A$ value for $KClO_4$ was here determined in complete analogy to PVC−NPOE membranes as −6.65 ± 0.02. This value, together

(24) Schaller, U.; Bakker, E.; Spichiger, U. E.; Pretsch, E. *Anal. Chem.* **1994**, *66*, 391.

(25) Telting-Diaz, M.; Bakker, E. *Anal. Chem.* **2001**, *73*, 5582.

(26) Ion, A. C.; Bakker, E.; Pretsch, E. *Anal. Chim. Acta* **2001**, *440*, 71.

with the known complex formation constant of valinomycin (K-1) in PVC−DOS[17] ($\beta_1 = 10.1$) gives an upper detection limit of log a_K(UDL) = −2.9 (eq 10). In contrast, the experimental upper detection limit (log a_K(UDL) = −1.8) was found to be higher (data not shown). Some of the assumptions used in developing eqs 9 and 10 are indeed inadequate for nonpolar membrane phases.

A number of papers have appeared that treat the effect of ion pair formation on the potentiometric characteristics of ion-selective electrodes.[12,27,28] Recently, Buhlmann et al. estimated from reasonably expected ion pair formation constants in PVC membranes that the upper detection limit may be shifted by up to ∼1 order of magnitude relative to a system where ion pair formation can be neglected.[12] The shift is perfectly in line with the deviation found above. To study these processes experimentally, we chose here a more direct method to illustrate the separate equilibrium processes that dictate the upper detection limit.

As established in the Theory section (eq 14), the upper detection limit can be equally determined by performing a sandwich membrane experiment, where one segment remains unperturbed by coextraction processes, while the other undergoes anion interference. The potential of such a membrane (eq 14) should be equivalent to the processes shown in eq 3 for the classical determination of the upper detection limit. The membrane potential for a valinomycin-based sandwich in contact with KCl on the left side (inner filling solution) and $KClO_4$ on the right side (sample side) was found to be −31 ± 2 mV, which translates to −275 ± 2 mV if the sample activities are extrapolated to 1 M with the Nernst equation. This potential corresponds to the difference in the intercepts of the two Nernstian portions of the calibration curves ($K_A - K_I$ in eq 3) and can be directly utilized to calculate the upper detection limit as log a_K(UDL) = −2.3. This value is now closer to that from the direct experiment (−1.8; see above). The observed discrepancy between the two values could be explained with the occurrence of a small junction potential between both membrane segments, although the experiments are very reproducible and the single-membrane experiments undergo similar gradients. Alternatively, the classical anion interference experiment is more likely performed under transient conditions, where the total phase boundary concentrations (L_T and R_T in eq 9) may not be equal to their bulk membranes values. This condition is fulfilled more likely with the sandwich experiment, where the individual segments are equilibrated with their respective solutions before measurement.

As discussed in the Theory section, the sandwich experiment noted with eq 14 can be broken up into a thermodynamic cycle of three individual sandwich membrane measurements that can each be experimentally evaluated. Experimental potentials were found to be 363 ± 3 mV for eq 19, −468 ± 4 mV for eq 20, and 69 ± 2 mV for eq 21. After extrapolating all aqueous ion activities to 1 M with the Nernst equation, the resulting potentials for all three experiments were calculated as 122 ± 3, −468 ± 4, and 69 ± 2 mV. The sum of the three values corresponds to −277 ± 3 mV, which is essentially identical to the potential, −275 ± 2 mV, for the direct sandwich experiment (eq 14; see above).

The thermodynamic cycle experiment shows that the principal processes governing the upper detection limit of PVC−DOS membranes are the same as for the simpler PVC−NPOE systems. The membranes are very hydrophobic, and electrolyte extraction is only a favored process if an ionophore is present that mediates the extraction of an ion by complexation. These two factors alone, however, cannot account quantitatively for the upper detection limit of PVC−DOS-based ISEs. Ideally, in the absence of any ion pair formation, eq 21 should give a 27.9-mV membrane potential since the left side contains a 3 times smaller net concentration of ion exchanger (5 mmol kg^{-1}) than the right side (15 mmol kg^{-1}). However, the 69 mV observed experimentally is larger. It suggests that ion pairs between the complexed potassium ion and the extracted perchlorate are weaker than the ion pairs formed with the lipophilic ion exchanger in the other segment. This was here confirmed independently by measuring the membrane potential of a sandwich that contained anion exchanger $TDMA^+$ on the left side and valinomycin on the right side, both in contact with potassium perchlorate. The observed membrane potential was 32 ± 1 mV. The weaker ion pair between perchlorate and the complexed potassium was therefore confirmed. This finding is perhaps not too surprising, since the tridodecylmethylammonium ion appears to be less sterically shielded than a complexed potassium ion, but it suggests that $TDMA^+$ is not an ideal nonspecific ion exchanger where ion pairing can be disregarded. The fact that this ion exchanger shows significant selectivity for heparin relative to more symmetrical quaternary ammonium salts supports this notion.[29]

Unfortunately, the relatively large experimental value for eq 21 makes it impossible to accurately predict upper detection limits for PVC−DOS membranes on the basis of complex formation constants and apparent coextraction constants alone. The extent of ion pair formation appears to be influenced by the chemical structure of the ion−ionophore complex, the magnitude of which would have to be evaluated separately for every ionophore. Nonetheless, it seems to be possible to perform targeted experiments to elucidate the contribution of each process by performing adequate sandwich membrane experiments.

CONCLUSIONS

The sandwich membrane technique is used to estimate the coextraction constants of the electrolytes into the plasticized PVC membranes with acceptable accuracy. For the simpler polar valinomycin-based PVC−NPOE membrane, the upper detection limits are predicted accurately from the stability constant of the ionophore, coextraction constants, and membrane compositions due to the neglected ion pairs. On the other hand, the upper detection limit of the nonpolar PVC−DOS membrane is more difficult to predict quantitatively. The sandwich membrane experiments show that the ion pairing between the ionophore−metal ion complexes and the extracted anion is weaker than the one between the lipophilic ion exchanger and the anion. Such experiments allow one, for the first time, to gain a more detailed, quantitative insight into the separate thermodynamic processes that govern the extraction of electrolyte into such ion sensing membranes.

(27) Egorov, V. V.; Lushchik, Y. F. *Talanta* **1990**, *37*, 461.
(28) Cobben, P. L. H. M.; Egberink, R. J. M.; Bomer, J. G.; Bergveld, P.; Reinhoudt, D. N. *J. Electroanal. Chem.* **1994**, *368*, 193.
(29) Fu, B.; Bakker, E.; Yang, V. C.; Meyerhoff, M. E. *Macromolecules* **1995**, *28*, 5834.

ACKNOWLEDGMENT

This research was financially supported by the National Institutes of Health (GM59716 and GM58589).

Received for review August 31, 2001. Accepted April 5, 2002.

AC0156159